https://doi.org/10.3311/PPch.40663
Creative Commons Attribution

Periodica Polytechnica Chemical Engineering, 69(3), pp. 457–469, 2025

Isotherm, Kinetic, and Thermodynamic Insights on Effective Sequestration of Cr(VI) by using De-oiled Karanja Seed Biochar

Sumalatha Boddu[1], Solomon Godwin Babu Neelamegam David[1], Jagadishwar Rao Gudipudi[1], Subbaiah Tondepu[1], Anoar Ali Khan[2], Ramesh Naidu Mandapati[1*]

[1] Department of Chemical Engineering, VFSTR (Deemed to be) University, Vadlamudi, 522213 Guntur, Andhra Pradesh, India
[2] Department of Chemical Engineering, Haldia Institute of Technology, 721657 Haldia, West Bengal, India
* Corresponding author, e-mail: drmrn_chem@vignan.ac.in

Received: 09 April 2025, Accepted: 05 August 2025, Published online: 12 September 2025

Abstract

This study investigates the potential of non-edible waste-derived Karanja seed (*Pongamia pinnata*) biochar (KSB) as a biosorbent for Cr(VI) removal from synthetic effluents. Characterization of KSB before and after Cr(VI) biosorption using thermogravimetric analysis, scanning electron microscopy/energy dispersive X-ray spectroscopy, X-ray diffraction, and Fourier-transform infrared spectroscopy confirmed that the adsorption process primarily occurs through chemisorption, ion exchange, and/or complexation mechanisms. The effects of several process parameters, including pH, contact time, initial Cr(VI) concentration, KSB dosage, and temperature, on Cr(VI) biosorption efficiency were systematically examined through batch experiments. The results indicated an optimum biosorption efficiency of 91% under the following conditions: initial Cr(VI) concentration of 20 mg L^{-1}, contact time of 60 min, pH 2, KSB loading of 0.01 g, and a temperature of 303 K. Adsorption equilibrium data were analyzed using the Freundlich and Langmuir isotherm models, with the Langmuir model yielding a maximum biosorption capacity of 164 mg g^{-1}, suggesting monolayer biosorption. Kinetic analysis demonstrated that the pseudo-second-order model provided the best fit, indicating that chemisorption governed Cr(VI) uptake on KSB, involving three distinct intra-particle diffusion stages. Thermodynamic parameters (ΔH^0, ΔG^0, and ΔS^0) were evaluated, confirming that the biosorption process was spontaneous, exothermic, and thermodynamically feasible. Additionally, the biosorption-desorption performance of KSB for Cr(VI) was assessed through cyclic experiments, highlighting its regeneration potential for practical applications. Finally, the results revealed that KSB is an efficient and cheap biosorbent for the sequestration of Cr (VI) from a synthetic medium.

Keywords

Karanja seed biochar, Cr(VI), biosorption, isotherms, kinetics

1 Introduction

Environmental contamination is a serious issue caused by urbanization, rapid population growth, industrialization, and globalization. Water pollution is one of the essential problems faced by living things due to the high discharge of contaminants such as heavy metals, pharmaceutical waste, and organic matter from these industries [1]. Heavy metals such as Cu, Cr, Zn, Cd, Pb, Pt, Fe, and Hg play an important role in polluting the water due to their unacceptable characteristics such as toxicity and persistency [2]. Since these heavy metals are not biodegradable, they tend to collect and eventually raise the concentrations in a body of water. Their deposition affects directly or indirectly to the living organisms due to biomagnification. The most dangerous and toxic metals are chromium, which has two oxidation states (Cr(III) and Cr(VI) ($Cr_2O_7^{2-}$)), and its composites. These metals are produced by a variety of anthropogenic resources, such as the leather and tanning process units, electroplating industry, dye, paint, and paper manufacturing, and the petroleum refining processes. These industries release both trivalent and hexavalent chromium. Among both chromium states, the Cr(VI) is considered as most harmful pollutant due to its high intake in industry. According to United States Environmental Protection Agency (USEPA) regulation, the maximum acceptable release of Cr(VI) into water bodies is 0.1 mg L^{-1} and the highest acceptable concentration of Cr(VI) is 0.05 mg L^{-1} in the effluent stream [3]. Wastewater must be treated before being released since exceeding the allowable limit of Cr(VI) can have serious health consequences, including cancer, mass loss, and kidney and liver damage [4]. The treatment includes several traditional

Cite this article as: Boddu, S., Neelamegam David, S. G. B., Gudipudi, J. R., Tondepu, S., Khan, A. A., Mandapati, R. N. "Isotherm, Kinetic, and Thermodynamic Insights on Effective Sequestration of Cr(VI) by using De-oiled Karanja Seed Biochar", Periodica Polytechnica Chemical Engineering, 69(3), pp. 457–469, 2025. https://doi.org/10.3311/PPch.40663

processes such as ion exchange, membrane filtration, precipitation, reverse osmosis, coagulation, oxidation, electrochemical treatment, and extraction, as they can remove toxic pollutants, but the application of these methods is not feasible economically as they are expensive, and some are unable at lower metal concentrations [5]. Biosorption is a promising technology that can be applied to treat wastewater efficiently with low cost and low energy consumption even if there is a low concentration of Cr(VI) released into the water bodies.

The biosorption technique involves the uptake of heavy metals from wastewater by biological materials through a physicochemical pathway. The physiochemical pathway includes treating biological materials to remove impurities to make a suitable sorbent to adsorb heavy metals such as Cr(VI), Pb, Cu, and As. The process involves a synthesis of biochar first as a biosorbent to remove the pollutant from the water surface. Biochar preparation takes place upon thermochemical conversion of biomass, where a thermal process such as pyrolysis at a quantified temperature is applied to biomass. Lignocellulose-based biosorbents, derived from agricultural wastes are usually most favorable as they are environment-friendly, economically viable, and show the effective sorption of organic and inorganic contaminants. There are many agricultural waste materials used as a biosorbent such as rice straw, tamarind peel, banana peel, acorn shell, mango seed, orange peel, cedar tree bark, plum tree bark, tree fruit shell, avocado peel, lemon coconut fiber, pineapple peels, and vanilla bean waste [6]. Karanja seed (*Pongamia pinnata*) an agro-industrial waste was considered for the efficient sequestration of Cr (VI) from the effluent streams.

Karanja is a non-edible oilseed crop acquired in India and found in Southeast Asia and Australia. Karanja trees serve as a potentially low-cost and easily available feedstock [7]. The Karanja seed contains oil (27–39%), protein (17–37%), starch (6–7%), crude fiber (5–7%), moisture (15–20%), and ash content (2–3%) [8]. The Karanja seed was considered biomass and was subjected to pyrolysis at a specified temperature for a certain hour to convert it into biochar.

This study's primary goal was to use Karanja seed biochar (KSB) as a biosorbent to efficiently adsorb the heavy metal Cr(VI) from wastewater. The contact time, dosage of biosorbent, concentration of Cr(VI) in water, and pH of Cr(VI) variations were considered to understand the efficient removal behavior of KSB. The KSB was characterized using thermogravimetric analysis (TGA), scanning electron microscopy/energy dispersive X-ray spectroscopy (SEM/EDS), Fourier-transform infrared spectroscopy (FTIR), X-ray diffraction (XRD), and a UV-visible (UV-Vis) spectrophotometry. TGA for thermal behavior, SEM/EDS for surface topology/morphology, FTIR for functional group identification, XRD for crystallographic structure and inorganic composition, and a UV-Vis spectrophotometer was used to find out the concentration of Cr(VI) present in wastewater. The adsorption isotherm was fitted to the Langmuir and Freundlich models, kinetic studies, and thermodynamic studies were also done to investigate the adsorption behavior and thermodynamic properties such as endothermic or exothermic behavior.

2 Materials and methods

2.1 Reagents and chemicals

The standard and test solutions were prepared ccording to the following description. Cr(VI standard solution (1000 mg L^{-1}) was prepared by dissolving the required amount of $K_2Cr_2O_7$ (Merck India Pvt. Ltd.) in 1000 mL of distilled water. Test solutions with concentrations ranging from 20 to 100 mg L^{-1} were prepared by diluting the stock solution with double-distilled water. The pH of the test solutions was adjusted to the desired value using 0.1 M HCl and 0.1 M NaOH. All chemicals were of analytical grade.

2.2 Synthesis of biomaterial

The de-oiled Karanja seed cake biomass, a residual byproduct derived from oil extraction, was acquired for subsequent processing. According to Nisar et al. [9], 40 g of biochar can be obtained from 100 g of biomass. The biomass underwent a washing process followed by air-drying over 12 days to achieve a less than 12% moisture content at 333 K. The dried biomass was mechanically comminuted using a mortar and subsequently sieved to obtain a uniform particle size distribution, a critical parameter for ensuring controlled thermal conversion. The processed biomass was carbonized in clay pots (180 mm × 75 mm), which were sealed with M-Seal to maintain airtight conditions. The clay pots were placed in a muffle furnace and heated to a target temperature 773 K at a controlled heating rate 283 K min^{-1}. The carbonization temperature and operational parameters were selected based on optimization studies reported in prior research [10]. After a residence time of 1 h at the target temperature, the muffle furnace was switched off and allowed to cool naturally. The resultant biochar was collected, sieved to achieve

uniform particle size, and subsequently stored for adsorption experiments.

2.3 Biomass characterization

Thermal stability of biochar was assessed using a simultaneous thermal analyzer (STA 7200, Hitachi HTG, Japan) in nitrogen atmosphere with a flow rate of 30 mL min^{-1}. The structural characteristics and phase fractions of the biosorbent were investigated using an X-ray diffractometer (Rigaku Miniflex 600, Rigaku Corporation, Japan). The topographical and elemental features were investigated using a scanning electron microscope (VEGA 3, SBH, TESCAN Brno S.R.O, Czech Republic) coupled with energy diffractive spectroscopy. The surface functional groups were determined using a FTIR spectrometer recorded in the range of 500–4000 cm^{-1} (Cary 630 FTIR with Diamond ATR, Agilent Technologies, USA).

2.4 Uptake measurements

The biosorption of Cr(VI) using KSB was investigated in batch mode under varying process parameters, including pH (1–8), contact time (1–120 min), initial Cr(VI) concentration (20–100 mg L^{-1}), biosorbent dosage (0.01–0.05 g), and temperature (303–333 K). Each experiment was conducted in a 250 mL conical flask containing 30 mL of Cr(VI) solution, agitated at 180 rpm in a shaking incubator (Model: 116736GB, GeNei, India). After the completion of the biosorption process, the Cr(VI)-loaded biosorbent was separated from the solution through filtration using Whatman No. 42 filter paper with a pore size of 0.45 µm. All experiments were performed in triplicate, and the average values were reported. Aliquots from the filtrate were analyzed for residual Cr(VI) concentrations using UV Spectroscopy (UV-2600, Shimadzu, Japan). The initial and final Cr(VI) concentrations in the solution were denoted as C_i and C_e (at 363 nm wavelength of the detection), respectively.

The efficiency of biosorption was calculated using Eq. (1):

$$\text{Efficiency of biosorption} = \frac{C_i - C_e}{C_i} \times 100. \quad (1)$$

The sorption capacity of KSB (q) was evaluated from the accompanying Eq. (2):

$$q = \frac{V \times (C_i - C_e)}{1000 \times w}, \quad (2)$$

where V is the volume of Cr(VI) (mL) and w is the KSB mass (g), C is the concentration of Cr(VI) (mg L^{-1}).

2.5 Equilibrium and thermodynamic study

To obtain the adsorption isotherms, 0.01 g of KSB was suspended in the Cr(VI) solutions with concentrations ranging from 20 to 100 mg L^{-1} at the optimum pH. To assess the effect of temperature on adsorption, isotherm experiments were conducted at four different temperatures in the 303–333 K range.

2.6 Kinetic study

The kinetics of Cr(VI) adsorption using KSB were examined at five initial concentrations (20, 40, 60, 80, and 100 mg L^{-1}) under optimum pH conditions and a constant temperature of 303 K. The efficiency of biosorption was evaluated at regular time intervals to determine the adsorption rate and mechanism.

2.7 Regeneration studies

The study evaluated the desorption and regeneration potential of KSB for Cr(VI) removal to restore its biosorption capacity. Desorption involves the release of biosorbed Cr(VI) ions from the exhausted KSB surface, enabling its reuse in multiple adsorption cycles. For the biosorption process, 0.01 g of KSB was introduced into 30 mL of Cr(VI) solution (20 mg L^{-1}) and agitated for 120 min. The mixture was then filtered, and the residual Cr(VI) concentration in the supernatant was determined using a UV-Vis spectrophotometer. The Cr(VI)-loaded KSB retained after filtration was thoroughly washed with distilled water to remove any loosely bound Cr(VI) ions and subsequently dried at 373 K for 12 h. To facilitate Cr(VI) desorption, the dried Cr(VI)-loaded KSB was immersed in 50 mL of 0.1N NaOH solution and agitated for 120 min. Following the desorption process, the solution was filtered, and the concentration of desorbed Cr(VI) was quantified. The desorption efficiency was determined using Eq. (3) to evaluate the regeneration potential of KSB for successive adsorption-desorption cycles [11–14].

$$\text{Desorption efficiency } (\%) = \frac{\text{amount of Cr(VI) ion desorbed}}{\text{amount of Cr(VI) ion adsorbed}} \quad (3)$$

3 Results

3.1 KSB characteristics

3.1.1 Thermogravimetry analysis of Karanja seed biomass

The TGA and derivative thermogravimetry (DTG) of Karanja seeds reveal their thermal degradation characteris-

tics over a temperature range of room temperature to 1073 K as shown in Fig. 1. The TGA of Karanja seed biomass reveals a three-stage thermal decomposition behavior typical of lignocellulosic materials. The initial mass loss observed below 423 K corresponds to the evaporation of moisture and low-boiling volatiles. A major mass loss occurs between 423 K and 623 K, attributed to the decomposition of hemicellulose and cellulose, with a prominent peak around 633 K in the DTG curve indicating the maximum rate of thermal degradation. In the final stage, lignin degrades gradually, contributing to a slower mass loss and resulting in a stable char residue beyond 633 K. Overall, the biomass exhibits a total mass loss of approximately 65–70%, leaving behind about 30–35% residual mass, which indicates a high fixed carbon content. These thermal characteristics suggest that Karanja seed biomass is a suitable feedstock for thermochemical conversion processes like pyrolysis or gasification, offering potential for bioenergy production and value-added carbon materials [11–13].

SEM-EDS studies

SEM and EDS analyses were conducted to evaluate the morphology and elemental composition of KSB before and after chromium adsorption. As shown in Fig. 2 (a), SEM analysis revealed that the biosorbent exhibited a highly heterogeneous structure with a rough and porous surface morphology, which is beneficial for adsorption. The EDS spectrum before the uptake measurements (Fig. 2 (a)) detected predominant elements such as C and O, confirming the organic nature of the biochar [15]. Following the biosorption of Cr(VI), the EDS analysis of KSB (Fig. 2 (b)) confirmed the presence of chromium on the sorbent surface, as evidenced by the distinct Cr peak in the spectrum. The surface appeared smoother due to metal deposition, further supporting the adsorption process. Additionally,

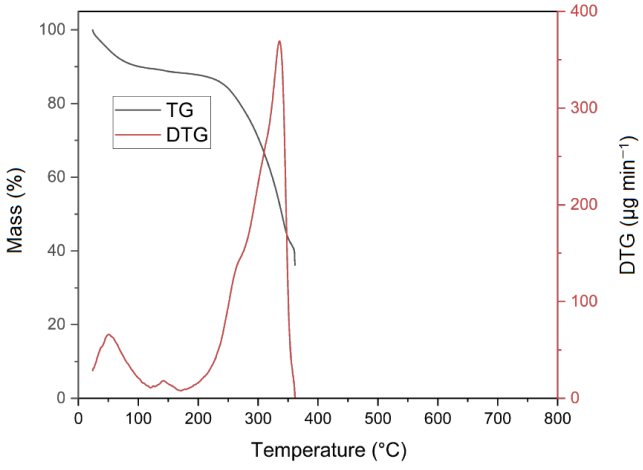

Fig. 1 Thermogravimetry analysis of Karanja seed biomass

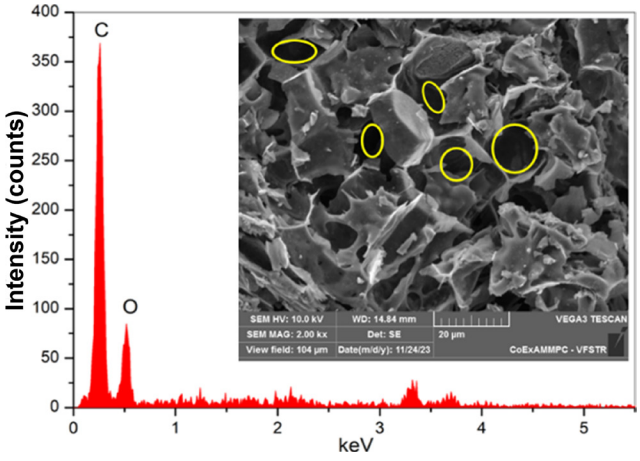

(a)

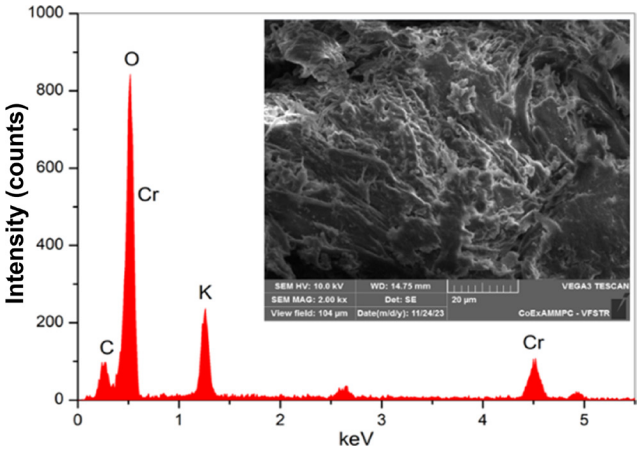

(b)

Fig. 2 SEM-EDS of (a) Virgin KSB and (b) Cr(VI) loaded KSB at a pH of 2.0

the observed increase in oxygen content may be attributed to the formation of Cr_2O_3 species during the interaction of chromium with biochar functional groups, which contributes to the higher oxygen signal in the system. These findings confirm the efficacy of KSB in removing Cr(VI) from aqueous solutions, highlighting its potential application in water purification and heavy metal remediation.

XRD studies

The XRD diffractogram of Cr(VI)-adsorbed KSB is presented in Fig. 3. The diffractogram exhibits a broad peak centered around $2\theta \approx 20–30°$, indicative of the amorphous nature of the biochar matrix. Notably, the presence of minor diffraction peaks within the 15–40° range can be attributed to adsorbed metal phases present in the biochar. The broad hump observed in the region between 20–30° is characteristic of amorphous carbon, which is commonly found in biomass-derived biochars due to incomplete graphitization. Additionally, the weak reflections beyond 40° indicate the presence of residual inorganic phases,

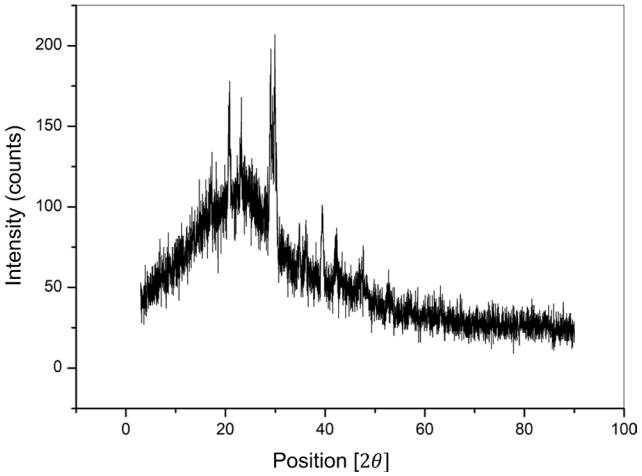

Fig. 3 XRD of Cr(VI) loaded KSB

possibly metal oxides formed during adsorption [16]. The XRD results confirm that the biochar remains largely amorphous, providing a high surface area favorable for metal adsorption. Overall, the XRD analysis supports the suitability of KSB as an effective biosorbent for Cr(VI) removal, with its amorphous carbon structure playing a significant role in metal ion binding.

FTIR studies

The functional groups located on the KSB are critical on the cell wall surface are critical for the adsorption of heavy metals. Fig. 4 displays the FTIR spectra of both untreated KSB and Cr(VI)-loaded KSB. A broad and intense absorption band at 3334 cm^{-1} suggests the presence of O−H alcohol functional groups, characterized by strong intensity and stretching vibrations. A distinct peak at 2894 cm^{-1} is attributed to the symmetrical stretching vibrations of $-CH_2$ alkane, commonly found

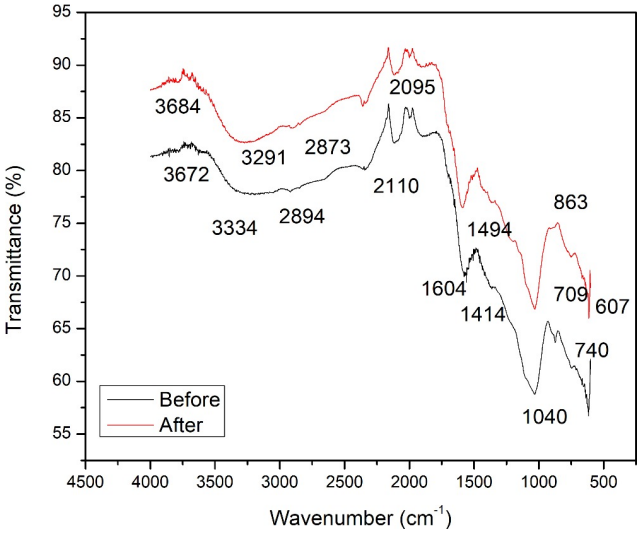

Fig. 4 FTIR of virgin KSB and Cr(VI) loaded KSB

in carbohydrate ring structures. The prominent band at 1604 cm^{-1} corresponds to the C=O stretching vibration, while the band at 1040 cm^{-1} is indicative of asymmetric C−O stretching and/or strong C−X stretching bonds. A less intense band at 1414 cm^{-1} is associated with the bending vibration of −C−H in the methylene group, and the band at 755 cm^{-1} is characteristic of C−X halide stretching. These findings confirm the existence of multiple ionizable functional groups, such as hydroxyl, amine, methyl, carbonyl, and carboxyl groups, on the biomass surface [17]. Following Cr(VI) biosorption, the broad peak shifted to 3291 cm^{-1}, aligning with the O−H functional group [18–20] exhibiting strong intensity stretching vibrations and/or N−H aromatic functional groups displaying medium to weak intensity stretching vibrations. The peak at 1494 cm^{-1} is linked to the C=C aromatic functional group, showing medium to weak intensity stretching vibrations. Furthermore, a new peak emerged at 863 cm^{-1}, indicating the presence of the =C−H alkene functional group with bending vibrations and strong intensity. A minor shift was observed at 709 cm^{-1}, and a peak at 607 cm^{-1} is associated with =C−H alkene and/or C−X alkyl halide functional groups, exhibiting strong intensity stretching vibrations. Finally, the small peak at 2873 cm^{-1} signifies the O−H acid functional group with strong or very broad intensity stretching vibrations and/or C−H alkane functional groups with strong intensity and stretching vibrations. Upon comparing the FTIR spectra of KSB before and after biosorption, it is evident that the biosorption process led to shifts in the bands towards higher wavenumbers. This shift is attributed to the formation of carboxylate, amine, amide, and hydroxylate anions during biosorption [21].

3.2 Factors influencing the efficiency of biosorption on KSB

3.2.1 Effect of pH

The pH of the solution is a crucial parameter influencing the biosorption process, as it impacts the biomass surface charge, the ionization state of functional groups, and the speciation of the biosorbate. To ensure statistical consistency and reproducibility, all preliminary experiments, including adsorption studies, were conducted in parallel using five identical samples of the same material under identical conditions. The data presented in the manuscript represent the average values of these parallel runs. The effect of pH on Cr(VI) biosorption by KSB was evaluated by adjusting the pH of the 20 mg L^{-1} Cr(VI) solution in the pH range 1–8, while maintaining a constant KSB concentration of 0.01 g in 30 mL^{-1}. The results, presented

in Fig. 5 (a), clearly demonstrate that the biosorption of Cr(VI) reaches its maximum at pH 2, with a subsequent decline as the pH increases. At lower pH, the dominant species of Cr(VI) is $HCrO_4^-$, which is favorable for biosorption. In contrast, at higher pH values, Cr(VI) exists predominantly as CrO_4^{2-} and $Cr_2O_7^{2-}$ ions, leading to reduced biosorption efficiency [22]. The decline in biosorption capacity with increasing pH is attributed to the competitive adsorption between CrO_4^{2-} and OH^- ions, with OH^- ions predominating at higher pH, thereby occupying available binding sites on the KSB surface. The maximum biosorption efficiency, as indicated in the study, was found to be 91% at pH 2.0. The point of zero charge (pH_{zpc}) is a crucial parameter in understanding the effect of solution pH on the biosorption efficiency. As shown in Fig. 5 (b), the pH_{zpc} [23] of KSB is 1.5. When the solution pH is below this value, the biosorbent surface becomes positively charged, which facilitates electrostatic attraction with anionic Cr(VI) ions such as $HCrO_4^-$ and $Cr_2O_7^{2-}$, resulting in higher biosorption rates under acidic conditions. In contrast, at pH values above the pH_{zpc}, the biosorbent surface acquires a negative charge, leading to electrostatic repulsion of these anionic Cr(VI) ions. Hence at pH 3, conditions are optimal for the biosorption of hexavalent Cr.

3.2.2 Contact time dependency

For efficient biosorption process design, the rate of adsorption is a critical factor. Fig. 5 (c) illustrates the impact of contact time on the biosorption efficiency of Cr(VI) using KSB. Initially, the biosorption efficiency increases rapidly within the first 10 min, reflecting the dominance of physical adsorption and ion exchange mechanisms between Cr(VI) ions and KSB. As the contact time increases, a slight rise in biosorption efficiency is observed, suggesting the involvement of additional mechanisms such as complexation and micro-precipitation, as reported in previous studies [24]. After reaching a peak efficiency, equilibrium is achieved, as the available active sites on the KSB surface (such as −COOH and −OH) become fully utilized. The biosorption efficiency reaches its maximum value within 60 min, beyond which no significant change in biosorption efficiency is observed, signifying that equilibrium has been attained. This rapid equilibrium indicates that KSB biomass is an effective biosorbent for the removal of Cr(VI) from industrial effluents.

3.2.3 Influence of Cr(VI) concentrations

Fig. 5 (d) presents the efficiency of biosorption at various Cr(VI) concentrations. It was noted that biosorption efficiency decreased as the initial concentrations increased. Such as, at an initial concentration of 20 to 100 mg L^{-1}, the efficiency of biosorption of Cr(VI) sorbed by KSB decreased from 96 to 68%. More efficiency of biosorption at low initial metal concentrations can be ascribed to the availability of vacant sites for metal binding [25]. As a result KSB is capable of binding Cr(VI) ions at various concentrations.

3.2.4 KSB loading capacity

Biosorbent loading is a critical factor in determining the biosorption capacity, as it influences the number of available binding sites for the biosorbate. The effect of KSB loading on the biosorption of Cr(VI) was investigated by varying the KSB concentration between 0.01 to 0.05 g L^{-1}, with a constant Cr(VI) concentration of 20 mg L^{-1}, pH 2, and a contact period of 60 min at room temperature. As shown in Fig. 5 (e), the biosorption efficiency increased with higher KSB loading, which corresponds to a greater number of available binding sites for Cr(VI) ions in solution. However, the uptake capacity of adsorbed per unit mass of adsorbent at a given time (q_t) decreased with increased biosorbent loading due to the incomplete saturation of binding sites, as reported by Semerjian et al. [26].

Furthermore, higher biosorbent concentrations can lead to particle aggregation, which reduces the available surface area and increases the diffusion path length, thus impairing the overall biosorption process. The observed decline in sorption capacity with increased biosorbent loading may also be attributed to reduced mixing efficiency at higher biosorbent densities and potential interference between binding sites, as suggested by Thangagiri et al. [22]. Based on these observations, a KSB loading of 0.01 g L^{-1} was selected for further experiments, as increasing the biosorbent dosage did not significantly enhance Cr(VI) removal efficiency.

3.3 Equilibrium modelling

Biosorption isotherms are essential for understanding the relationship between the concentration of the adsorbate in the solution and the amount of adsorbate adsorbed by the biosorbent at a constant temperature. In the context of heavy metal biosorption, isotherm studies provide valuable insight into the efficiency of biosorbents and help in designing appropriate industrial-scale adsorption systems. Various isotherm models, as presented in Table 1, were utilized to analyze the biosorption of Cr(VI) using KSB.

Fig. 6 (a) and (b) illustrates the experimental data for Langmuir and Freundlich isotherms, respectively. The isotherm model that best fit the experimental data was

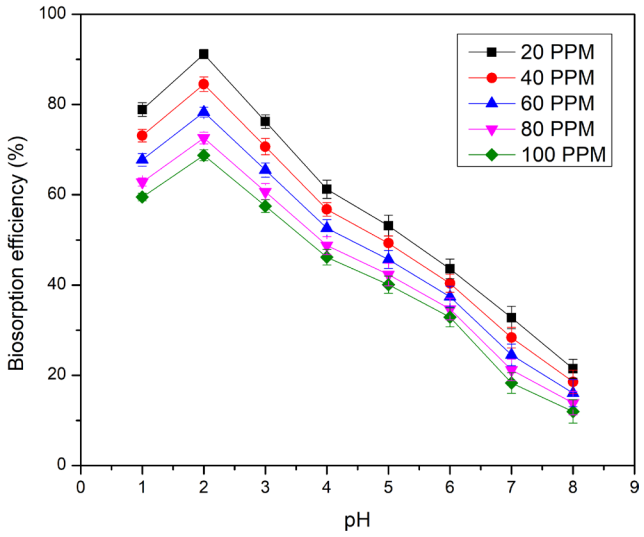

(a)

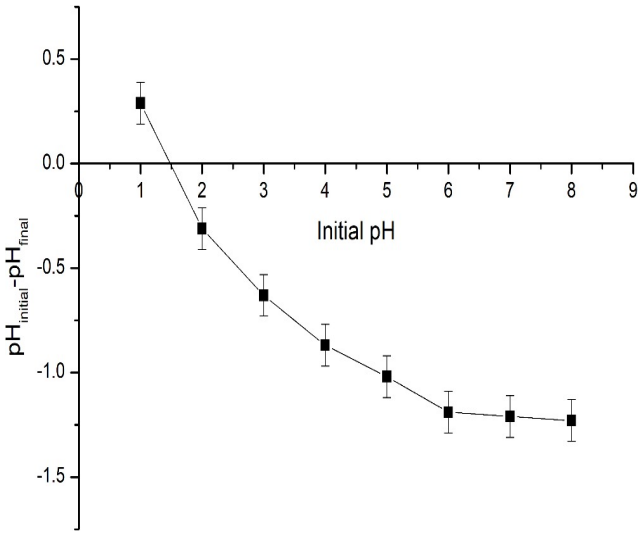

(b)

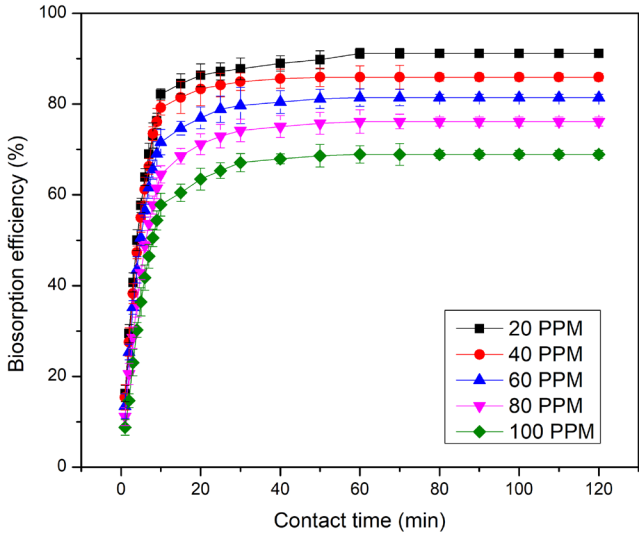

(c)

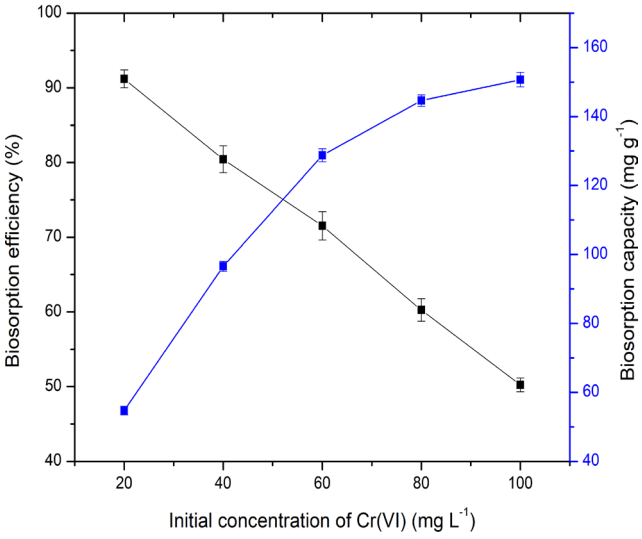

(d)

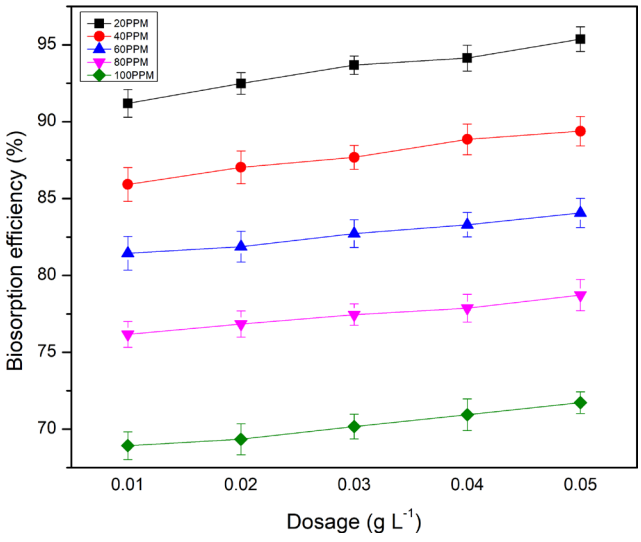

(e)

Fig. 5 Effect of (a) pH; (b) Point of zero charge; (c) Contact time; (d) Initial concentration; (e) KSB loading capacity of Cr(VI) onto adsorption on KSB

Table 1 Isotherm parameters of Cr(VI) adsorption on KSB at 303 K

Isotherms	Linear version of equation	Constants and coefficients of isotherms	
Langmuir	$\frac{C_e}{q_e}=\frac{C_e}{Q_L}+\frac{1}{Q_L K_L}$	Q_L (mg g^{-1})	163
		K_L (L mg^{-1})	0.22
		R^2	0.99
Freundlich	$\ln q_e=\ln K_f+\frac{1}{n}\ln C_e$	K_f (mg g^{-1})	18.19
		n (mg L^{-1})	0.15
		R^2	0.96

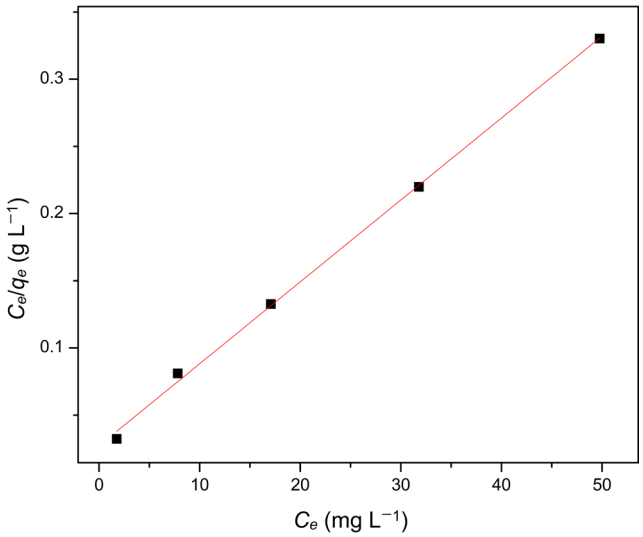

(a)

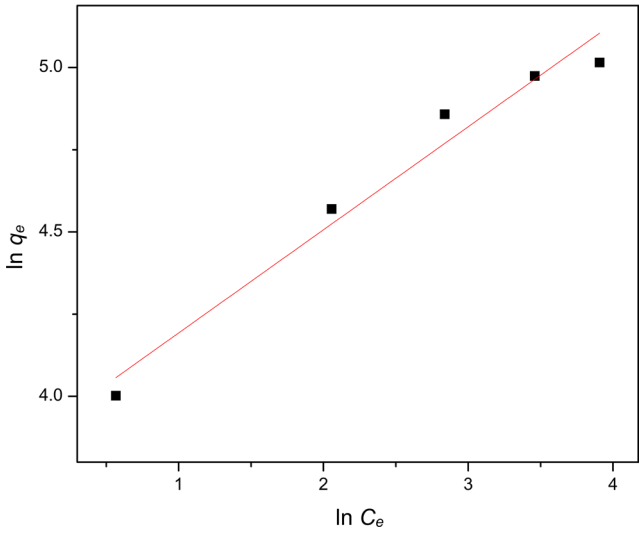

(b)

Fig. 6 Isotherm models for the removal of Cr(VI) using KSB: (a) Langmuir isotherm; (b) Freundlich isotherm

selected based on the coefficient of determination (R^2). According to the results, the Langmuir isotherm showed the best fit, with an R^2 value indicating a high correlation between the experimental data and the model. This suggests that Cr(VI) was adsorbed onto the KSB surface in a monolayer configuration, with a maximum uptake capacity of 163 mg g^{-1} [27].

The Freundlich isotherm, shown in Fig. 6 (b), also demonstrated a good fit with the experimental data, exhibiting an R^2 value of 0.96. The parameters of the Freundlich model are provided in Table 1. Both the Langmuir and Freundlich isotherms indicated that the equilibrium data can be well explained, with the Freundlich model highlighting the heterogeneous nature of the biosorption of Cr(VI) onto KSB.

3.4 Thermodynamic studies

Temperature significantly influences the dispersion behavior of adsorbate molecules on the adsorbent, thereby affecting adsorption capacity. The adsorption characteristics of Cr(VI) on KSB at varying temperatures (303, 313, 323, and 333 K) are presented in Fig. 7. An inverse relationship was observed between temperature and Cr(VI) adsorption efficiency, with adsorption capacity decreasing as temperature increased. At an initial Cr(VI) concentration of 20 mg L^{-1} in simulated wastewater, the adsorption capacity of KSB was 91 mg g^{-1} at 303 K. However, at 333 K, the adsorption capacity declined to 76 mg g^{-1}. This reduction in adsorption efficiency at elevated temperatures can be attributed to the inhibition of electrostatic interactions between Cr(VI) and KSB [1]. Additionally, higher temperatures resulted in a decreased diffusion rate of Cr(VI) since, its limit their access to the active binding sites of KSB and reducing overall adsorption performance.

The thermodynamic parameters of the biosorption process, namely ΔG, ΔH, and ΔS, were determined using experimental data and evaluated through the application of Eqs. (4) and (5).

$$\Delta G^0 = -RT\ln K_D, \tag{4}$$

$$\ln K_D = \frac{\Delta S^0}{R} - \frac{\Delta H^0}{RT}, \tag{5}$$

where T represents the absolute temperature (K), K_D represents the equilibrium constant, R represents the universal gas constant (8.314 J mol$^{-1}\cdot$K^{-1}), ΔG^0 indicates the standard temperature (303–273 K), ΔH^0 is the standard enthalpy change, ΔS^0 denotes the standard entropy change, and T denotes temperature.

The thermodynamic parameters were determined using the slope and intercept of the linear van't Hoff equation ($\ln K_D$ vs $1/T$). K_D was deduced experimentally using the ratio q_e/C_e at equilibrium for different temperatures (303, 313, 323, and 333 K) are presented in Fig. 7 (a).

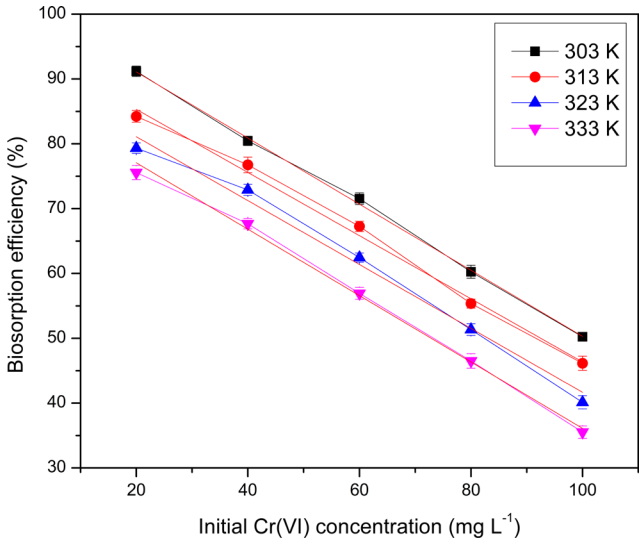

(a)

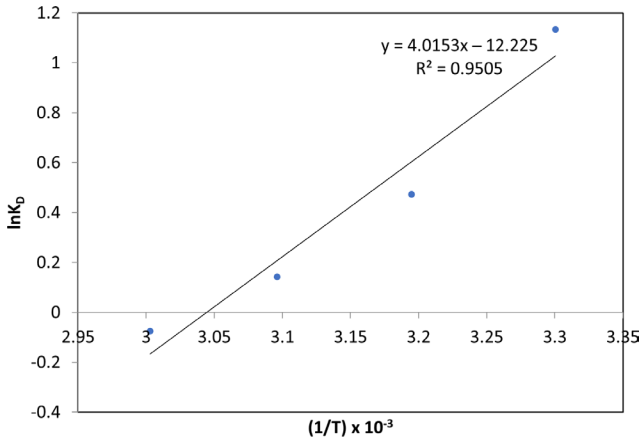

(b)

Fig. 7 Thermodynamic studies: (a) Effect of initial Cr(VI) concentration over temperature; (b) Plot of ln K_D vs $1/T$

The linear van't Hoff plot for Cr(VI) adsorption onto KSB at an initial Cr(VI) concentration of 20 mg L^{-1} is depicted in Fig. 7(b), with the corresponding thermodynamic parameters summarized in Table 2. The experimental data exhibited strong linearity, as indicated by a high correlation coefficient (R^2 = 0.925), suggesting a good fit to the model. The negative values of enthalpy change (ΔH) and entropy change (ΔS) confirm that the adsorption process is exothermic and associated with a reduction in system randomness. Furthermore, the Gibbs free energy (ΔG) values decreased with increasing temperature, indicating that the sorption process was more favorable at lower temperatures [28]. Considering wastewater temperature conditions, economic feasibility, and practical applications, 303 K was identified as the optimal temperature for adsorption.

Table 2 Thermodynamic parameters for biosorption of Cr(VI) onto KSB

S. No.	T (K)	ΔG^0 (kJ mol^{-1})	ΔH^0 (kJ mol^{-1})	ΔS^0 (J $mol^{-1}{\cdot}K^{-1}$)
1	303	−2854.03	−33.4	−101.6
2	313	−1227.88		
3	323	−379.62		
4	333	−207.18		

3.5 Kinetic modelling

Kinetic modeling of biosorption is crucial for scaling up the process for industrial applications. It provides insight into the reaction mechanisms, progression, and resistance encountered during mass transfer, as well as diffusion coefficients. To better understand the kinetics of Cr(VI) biosorption, a study was conducted using a 20 mg L^{-1} Cr(VI) solution at the optimal pH and a temperature of 303 K. The experimental data were analyzed using several kinetic models, including the pseudo-first-order, pseudo-second-order, intraparticle diffusion, and Elovich models (Table 3).

The experimental data aligned more accurately with the pseudo-second-order kinetic model, displaying poor fit with the pseudo-first-order kinetic model, as depicted in Fig. 8 (a) and (b). The associated kinetic parameters are listed with corresponding kinetic parameters in Table 3. Notably, the pseudo-second-order model provided a near fit, with the highest regression coefficient (R^2 = 0.997), suggesting that the biosorption of Cr(VI) onto KSB follows a chemisorption mechanism. This implies that the process involves chemical interactions between the adsorbate and the biosorbent [29].

Intraparticle diffusion analysis, shown in Fig. 8 (c), revealed three distinct linear phases, indicating that multiple kinetic stages govern the biosorption process. The first phase corresponds to the rapid diffusion of Cr(VI) ions to the exterior surface of KSB (instant biosorption). The second phase

Table 3 Kinetic parameters of Cr(VI) on KSB*

Model	Linear equation	Kinetic constants and coefficients	
Pseudo kinetic first order	$\ln(q_e - q_t) = \ln(q_e) - k_1 t$	$q_{e,\text{-exp}}$ (mg g^{-1})	54.71
		$q_{e,\text{-cal}}$ (mg g^{-1})	28.45
		k_1 (min^{-1})	0.10
		R^2	0.94
Pseudo kinetic second order	$\frac{t}{q_t} = \frac{1}{k_2 q_e^2} + \frac{1}{q_e} t$	k_2 (g mg^{-1} min^{-1})	0.01
		$q_{e,\text{-cal}}$ (mg g^{-1})	56.4
		$q_{e,\text{-exp}}$ (mg g^{-1})	54.71
		R^2	0.99
Elovich [23]	$q_e = B \ln A + B \ln t$	A (mg g^{-1} min^{-1})	11.06
		B (mg g^{-1})	8.5
		R^2	0.82

* In Table 3 exp means experimetal, cal means calculated, A is the initial adsorbed amout and B is the desorption constant.

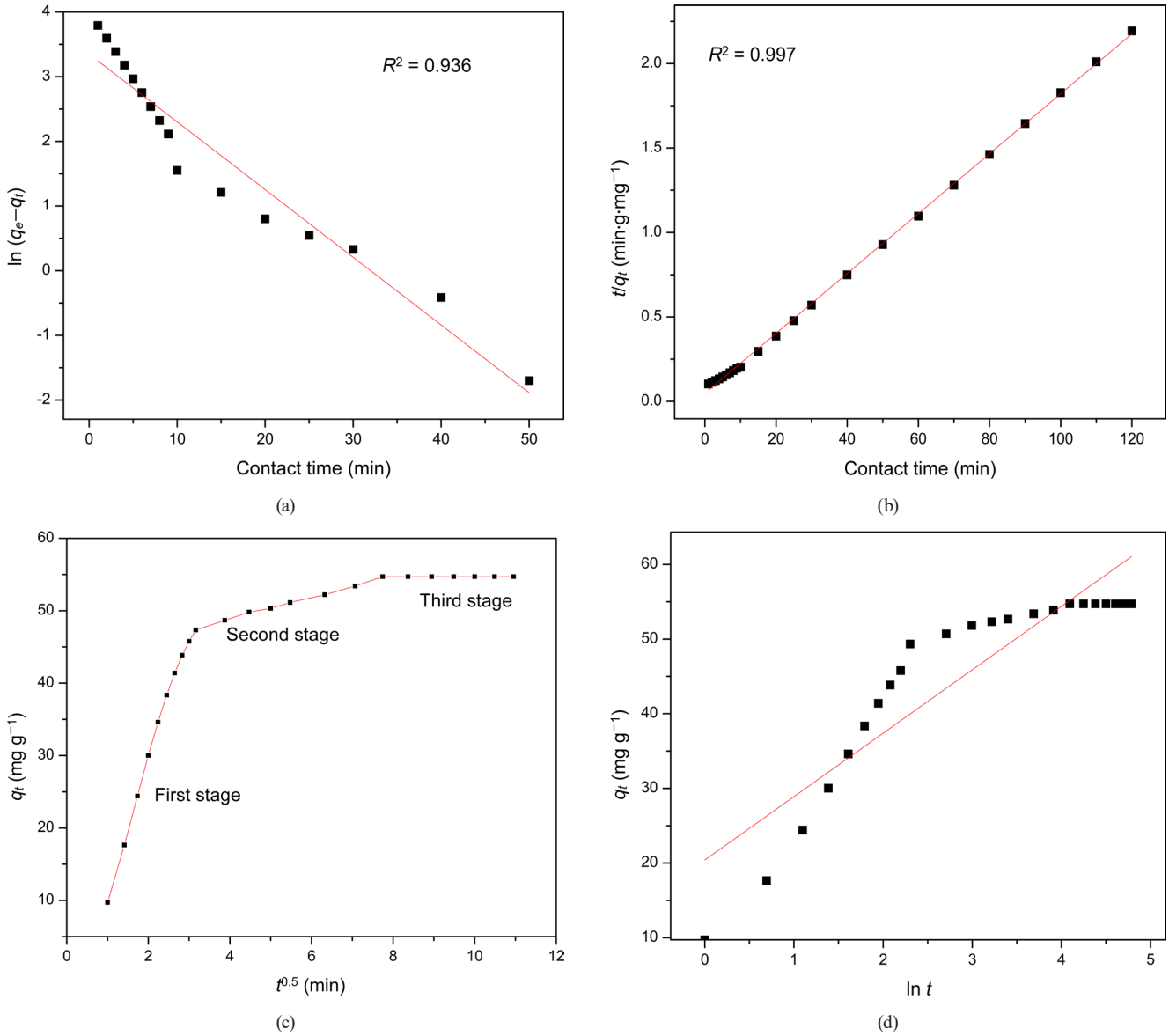

Fig. 8 Kinetic studies of Cr(VI) removal using KSB at room temperature: (a) Pseudo first order; (b) Pseudo second order; (c) Intra particle; (d) Elovich model for biosorption of Cr(VI) on KSB

represents the gradual biosorption associated with film diffusion, while the third phase signifies the slow approach to equilibrium, corresponding to surface diffusion. The graph did not pass through the origin, indicating that the biosorption of Cr(VI) onto KSB is not solely governed by pore diffusion, but is also influenced by boundary layer diffusion [30].

Furthermore, the experimental data were also fitted to the Elovich model, which supported the chemisorption nature of the biosorption process [31] The high regression coefficients (R^2) demonstrated the strong predictability of the model for Cr(VI) removal using KSB. Among the four kinetic models tested, the pseudo-second-order model was found to be the most suitable for describing the biosorption of Cr(VI) onto KSB.

3.6 Reusability of biosorbent

The biosorption process presents a significant advantage in wastewater treatment due to its reversibility through desorption, allowing for the regeneration and repeated use of the biosorbent. To assess the feasibility of continuous biosorbent application, the study evaluated the reusability performance of Cr(VI)-loaded KSB through regeneration trials. The regeneration of spent biosorbents is critical for large-scale industrial applications, as it enables repeated utilization while reducing overall treatment costs. The Cr(VI) adsorption-desorption cycles were conducted over five successive cycles, with the corresponding results illustrated in Fig. 9. A progressive decline in removal efficiency was observed with each cycle; however,

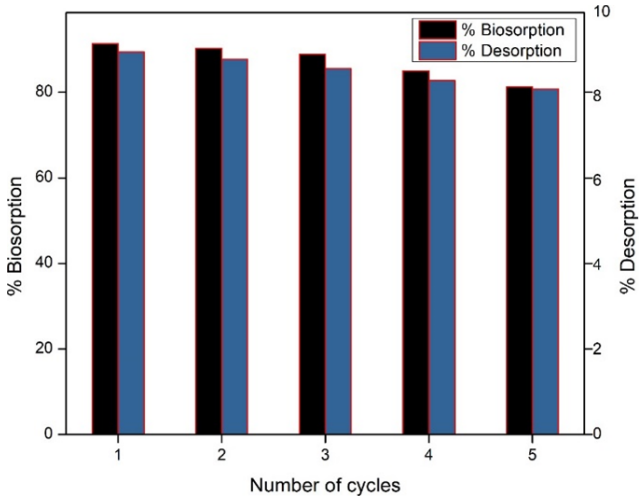

Fig. 9 Biosorption-desorption study of KSB

KSB retained approximately 80% efficiency after five cycles. The reduction in adsorption performance may be attributed to alterations in the physicochemical properties of KSB, particularly the gradual depletion of active binding sites due to the blockage of oxygen-containing functional groups [32]. Despite this decline, the study confirms that five adsorption-desorption cycles were effective, demonstrating that KSB is an environmentally viable biosorbent for Cr(VI) removal from aqueous systems.

3.7 Comparison of adsorption capacity of Cr(VI) for some adsorbents stated in literature

Comparison of KSB with different sorbents as shown in Table 4 [23, 33–39]. It was notified that the prepared KSB was a promising biosorbent for the biosorption of Cr(VI).

Table 4 Comparison of different adsorbents for Cr(VI) removal with their adsorption capacity

Adsorbent	Adsorption capacity (mg g^{-1})	Reference
Bagasse magnetic biochar	29.08	[33]
Magnetic modified-corncob biochar	25.94	[34]
Biochar-derived rice husk	4.46	[35]
Green waste biochar (mixture of maple, elm, oak wood chips and barks)	95	[36]
Corn straw biochar	90	[37]
Rosa Damascenaphytomass	140	[38]
Nostoc sp.	23.94	[39]
Turbinaria vulgaris	21.8	[39]
Spongomorpha indica	83.34	[23]
KSB	163.9	Present study

The adsorption efficiency of Cr(VI) removal using KSB was evaluated and compared with other adsorbents reported in prior studies, as summarized in Table 4. The findings from this investigation demonstrate that KSB exhibits superior effectiveness in Cr(VI) removal compared to the alternative adsorbents analyzed.

4 Conclusions

KSB waste biomass has demonstrated strong potential as an effective biosorbent for Cr(VI) removal from synthetic effluents. SEM-EDS analysis confirmed the porous nature of KSB, with its surface fully covered by Cr(VI) ions, aligning with EDS and XRD findings. FTIR analysis identified key functional groups, including hydroxyl, carboxyl, and amine, which play a crucial role in the biosorption process. The porous structure observed in SEM imaging enhances KSB's surface area, facilitating greater interaction with Cr(VI) ions. EDS analysis further verified the presence of essential elements such as oxygen and carbon, contributing to the material's biosorption capacity. In batch-mode experiments, KSB achieved a maximum biosorption efficiency of 91.18% for Cr(VI), with a metal uptake capacity of 163.93 mg g^{-1} under optimal conditions: pH 2, an initial metal concentration of 20 mg L^{-1}, a biosorbent dose of 0.01 g, and a temperature of 303 K. The adsorption process was best described by the Langmuir isotherm model, with a high correlation coefficient (R^2 = 0.9982), indicating monolayer adsorption on the KSB surface. The maximum monolayer adsorption efficiency was determined to be 22.67 mg g^{-1}. Kinetic studies revealed that the biosorption followed a pseudo-second-order model, with a regression coefficient (R^2 = 0.9982), confirming that chemisorption governed the process. Thermodynamic analysis indicated the exothermic nature of Cr(VI) adsorption onto KSB, with the following thermodynamic parameters: $\Delta G^0 = -2854.03$ kJ mol^{-1}, $\Delta H^0 = -33.4$ kJ mol^{-1}, and $\Delta S^0 = -101.6$ kJ mol^{-1}. These findings confirm that the biosorption process is spontaneous and thermodynamically favorable at lower temperatures. Further, a minimal loss in adsorption capacity after five cycles highlights the sustainability and reusability of KSB as a biosorbent. Overall, this study establishes KSB waste biomass as an effective, low-cost, and environmentally sustainable biosorbent for heavy metal removal from industrial effluents, particularly Cr(VI), offering a promising solution for wastewater treatment.

References

[1] Kumar, S., Shahnaz, T., Selvaraju, N., Rajaraman, P. V. "Kinetic and thermodynamic studies on biosorption of Cr(VI) on raw and chemically modified *Datura stramonium* fruit", Environmental Monitoring and Assessment, 192(4), 248, 2020. https://doi.org/10.1007/s10661-020-8181-x

[2] Zamora-Ledezma, C., Negrete-Bolagay, D., Figueroa, F., Zamora-Ledezma, E., Ni, M., Alexis, F., Guerrero, V. H. "Heavy metal water pollution: A fresh look about hazards, novel and conventional remediation methods", Environmental Technology & Innovation, 22, 101504, 2021. https://doi.org/10.1016/j.eti.2021.101504

[3] Boddu, S., Alugunulla, V. N., Dulla, J. B., Chavali, M., Pilli, R. R., Khan, A. A. "Estimation of biosorption characteristics of chromium (VI) from aqueous and real tannery effluents by treated *T. vulgaris*: experimental assessment and statistical modelling", International Journal of Environmental Analytical Chemistry, 102(16), pp. 4842–4861, 2022. https://doi.org/10.1080/03067319.2020.1789617

[4] Srivastava, S., Agrawal, S. B., Mondal, M. K. "Synthesis, characterization and application of *Lagerstroemia speciosa* embedded magnetic nanoparticle for Cr(VI) adsorption from aqueous solution", Journal of Environmental Sciences, 55, pp. 283–293, 2017. https://doi.org/10.1016/j.jes.2016.08.012

[5] Prasad, S., Yadav, K. K., Kumar, S., Gupta, N., Cabral-Pinto, M. M. S., Rezania, S., Radwan, N., Alam, J. "Chromium contamination and effect on environmental health and its remediation: A sustainable approaches", Journal of Environmental Management, 285, 112174, 2021. https://doi.org/10.1016/j.jenvman.2021.112174

[6] Ali Khan, A., Boddu, S., Halder, G. "Sustainable removal of Cr(VI) from wastewater by *Peltophorum pterocarpum* leaf powder", Materials Today: Proceedings, 57, pp. 1585–1592, 2022. https://doi.org/10.1016/j.matpr.2021.12.174

[7] Sharma, A., Kaushik, N., Rathore, H. "Karanja (*Milletia pinnata* (L.) Panigrahi): a tropical tree with varied applications", Phytochemistry Reviews, 19(3), pp. 643–658, 2020. https://doi.org/10.1007/s11101-020-09670-z

[8] Goskula, S., Siliveri, S., Gujjula, S. R., Adepu, A. K., Chirra, S., Narayanan, V. "Development of activated sustainable porous carbon adsorbents from Karanja shell biomass and their CO_2 adsorption", Biomass Conversion and Biorefinery, 14(24), pp. 32413–32425, 2024. https://doi.org/10.1007/s13399-023-05198-2

[9] Nisar, J., Waris, S., Shah, A., Anwar, F., Ali, G., Ahmad, A., Muhammad, F. "Production of Bio-Oil from De-Oiled Karanja (*Pongamia pinnata* L.) Seed Press Cake via Pyrolysis: Kinetics and Evaluation of Anthill as the Catalyst", Sustainable Chemistry, 3(3), pp. 345–357, 2022. https://doi.org/10.3390/suschem3030022

[10] Gunti, H., Kandukuri, D. J., Kumari, A., Aniya, V., Satyavathi, B., Naidu, M. R. "A non-edible waste as a potential sorptive media for removal of herbicide from the watershed", Journal of Hazardous Materials, 390, 121671, 2020. https://doi.org/10.1016/j.jhazmat.2019.121671

[11] Sidi-Yacoub, B., Oudghiri, F., Belkadi, M., Rodríguez-Barroso, R. "Characterization of lignocellulosic components in exhausted sugar beet pulp waste by TG/FTIR analysis", Journal of Thermal Analysis and Calorimetry, 138(2), pp. 1801–1809, 2019. https://doi.org/10.1007/s10973-019-08179-8

[12] Li, M., Wang, L., Li, D., Cheng, Y.-L., Adhikari, B. "Preparation and characterization of cellulose nanofibers from de-pectinated sugar beet pulp", Carbohydrate Polymers, 102, pp. 136–143, 2014. https://doi.org/10.1016/j.carbpol.2013.11.021

[13] Vieira, M. G. A., de Almeida Neto, A. F., Carlos da Silva, M. G., Nóbrega, C. C., Melo Filho, A. A. "Characterization and use of in natura and calcined rice husks for biosorption of heavy metals ions from aqueous effluents", Brazilian Journal of Chemical Engineering, 29(3), pp. 619–633, 2012. https://doi.org/10.1590/S0104-66322012000300019

[14] Katika, R. M., Boddu, S., Mandapati, R. N. "Enhanced Photodegradation of Congo Red Using RSM-Optimized TiO_2 on *Borassus flabellifer* Male Inflorescence Biochar", ChemistrySelect, 9(41), e202403454, 2024. https://doi.org/10.1002/slct.202403454

[15] Boddu, S., Narayana Alugunulla, V., Babu Dulla, J., Ali Khan, A., Babu Kolimarla, B., Jajula, S. "Enhanced biosorption of Cr(VI) from contaminated water using biodegradable natural polymeric biosorbent", Materials Today: Proceedings, 72, pp. 441–450, 2023. https://doi.org/10.1016/j.matpr.2022.08.312

[16] Kanagaraj, R., Nam, Y.-S., Pai, S. J., Han, S. S., Lee, K.-B. "Highly selective and sensitive detection of Cr^{6+} ions using size-specific label-free gold nanoparticles", Sensors and Actuators B: Chemical, 251, pp. 683–691, 2017. https://doi.org/10.1016/j.snb.2017.05.089

[17] Masuku, M., Nure, J. F., Atagana, H. I., Hlongwa, N., Nkambule, T. T. I. "Pinecone biochar for the Adsorption of chromium (VI) from wastewater: Kinetics, thermodynamics, and adsorbent regeneration", Environmental Research, 258, 119423, 2024. https://doi.org/10.1016/j.envres.2024.119423

[18] Solomon Godwin Babu, N. D., Ponnam, V., Tondepu, S. "Synthesis of Magnesium Titanate from Magnesium Chloride a Byproduct of Zirconium Plant", Journal of Sustainable Metallurgy, 2025. https://doi.org/10.1007/s40831-025-01145-9

[19] Pokuri, P., Ponnam, V., Ponnam, V. K. B., Neelamegam David, S. G. B., Tondepu, S. "Kinetic and Chemical Analysis of Pyrolysis in *Bambusa vulgaris* Leaves and Derived Fibers", Periodica Polytechnica Chemical Engineering, 68(4), pp. 587–596, 2024. https://doi.org/10.3311/PPch.37752

[20] Solomon Godwin Babu, N. D., Ponnam, V., Sharmila, S., Nagesh Chaganti, R. V. S., Tondepu, S. "A facile co-precipitation approach for the synthesis of high-pure magnesium titanate using sea water bitterns and titanium tetrachloride", Canadian Metallurgical Quarterly: The Canadian Journal of Metallurgy and Materials Science 64(3), pp. 1502–1509, 2025. https://doi.org/10.1080/00084433.2024.2397606

[21] Taher, T., Munandar, A., Mawaddah, N., Syamsuddin Wisnubroto, M., Siregar, P. M. S. B. N., Palapa, N. R., Wibowo, Y. G. "Synthesis and characterization of montmorillonite – Mixed metal oxide composite and its adsorption performance for anionic and cationic dyes removal", Inorganic Chemistry Communications 147, 110231, 2023. https://doi.org/10.1016/j.inoche.2022.110231

[22] Thangagiri, B., Sakthivel, A., Jeyasubramanian, K., Seenivasan, S., Raja, J. D., Yun, K. "Removal of hexavalent chromium by biochar derived from *Azadirachta indica* leaves: Batch and column studies", Chemosphere, 286, 131598, 2022. https://doi.org/10.1016/j.chemosphere.2021.131598

[23] John Babu, D., Sumalatha, B., Venkata Narayana, A., Venkateswrulu, T. C., Vidya Prabhakar, K., Abraham Peele, K. "Green treatment of chromium contaminated water using *Spongomorpha indica*", Regional Studies in Marine Science, 48, 102019, 2021. https://doi.org/10.1016/j.rsma.2021.102019

[24] Ehsanpour, S., Riahi Samani, M., Toghraie, D. "Removal of chromium (VI) from aqueous solution using Eggshell/ poly pyrrole composite", Alexandria Engineering Journal, 64, pp. 581–589, 2023. https://doi.org/10.1016/j.aej.2022.09.018

[25] Kumar, S., Narayanasamy, S., Venkatesh, R. P. "Removal of Cr(VI) from synthetic solutions using water caltrop shell as a low-cost biosorbent", Separation Science and Technology, 54(17), pp. 2783–2799, 2019. https://doi.org/10.1080/01496395.2018.1560333

[26] Semerjian, L. "Removal of heavy metals (Cu, Pb) from aqueous solutions using pine (*Pinus halepensis*) sawdust: Equilibrium, kinetic, and thermodynamic studies", Environmental Technology & Innovation, 12, pp. 91–103, 2018. https://doi.org/10.1016/j.eti.2018.08.005

[27] Belattmania, Z., El Atouani, S., Kaidi, S., Bentiss, F., Tahiri, S., Reani, A., Sabour, B. "Protonated Biomass of the Brown Seaweed *Cystoseira tamariscifolia*: A Potential Biosorbent for Toxic Chromium Ions Removal", Research Journal of Environmental Sciences, 12(3),pp. 106–113, 2018. https://doi.org/10.3923/rjes.2018.106.113

[28] Boddu, S., Dulla, J. B., Alugunulla, V. N., Khan, A. A. "An assessment on removal performance of arsenic with treated *Turbinaria vulgaris* as an adsorbent: Characterization, optimization, isotherm, and kinetics study", Environmental Progress & Sustainable Energy, 39(2), e13313, 2020. https://doi.org/10.1002/ep.13313

[29] Alrowais, R., Bashir, M. T., Khan, A. A., Bashir, M., Abbas, I., Abdel Daiem, M. M. "Adsorption and Kinetics Modelling for Chromium (Cr^{6+}) Uptake from Contaminated Water by Quaternized Date Palm Waste", Water, 16(2), 294, 2024. https://doi.org/10.3390/w16020294

[30] Dulla, J. B., Tamana, M. R., Boddu, S., Pulipati, K., Srirama, K. "Biosorption of copper(II) onto spent biomass of *Gelidiella acerosa* (brown marine algae): optimization and kinetic studies", Applied Water Science, 10(2), 56, 2020. https://doi.org/10.1007/s13201-019-1125-3

[31] Babu, D. J., Sumalatha, B., Venkateswarulu, T. C., Das, K. M., Kodali, V. P. "Kinetic, Equilibrium and Thermodynamic Studies of Biosorption of Chromium (VI) from Aqueous Solutions using *Azolla Filiculoidus*", Journal of Pure and Applied Microbiology, 8(4), pp. 3107–3116, 2014. [online] Available at: https://www.researchgate.net/publication/268152347_Kinetic_Equilibrium_and_Thermodynamic_Studies_of_Biosorption_of_Chromium_VI_from_Aqueous_Solutions_using_Azolla_filiculoidus [Accessed: 08 April 2025]

[32] Boddu, S., Dulla, J. B., Alugunulla, V. N., Malladi, S., Kavitha, G., Khan, A. A. "Prospective removal characteristics of noxious cationic dye using Cladophora catenata: a sustainable approach", International Journal of Environmental Analytical Chemistry, 104(19), pp. 8050–8070, 2024. https://doi.org/10.1080/03067319.2023.2191319

[33] Liang, M., Ding, Y., Zhang, Q., Wang, D., Li, H., Lu, L. "Removal of aqueous Cr(VI) by magnetic biochar derived from bagasse", Scientific Reports, 10(1), 21473, 2020. https://doi.org/10.1038/s41598-020-78142-3

[34] Hoang, L. P., Van, H. T., Nguyen, L. H., Mac, D.-H., Vu, T. T., Ha, L. T., Nguyen, X. C. "Removal of Cr(VI) from aqueous solution using magnetic modified biochar derived from raw corncob", New Journal of Chemistry, 43(47), pp. 18663–18672, 2019. https://doi.org/10.1039/C9NJ02661D

[35] Sarkar, A., Ranjan, A., Paul, B. "Synthesis, characterization and application of surface-modified biochar synthesized from rice husk, an agro-industrial waste for the removal of hexavalent chromium from drinking water at near-neutral pH", Clean Technologies and Environmental Policy, 21(2), pp. 447–462, 2019. https://doi.org/10.1007/s10098-018-1649-5

[36] Zheng, W., Guo, M., Chow, T., Bennett, D. N., Rajagopalan, N. "Sorption properties of greenwaste biochar for two triazine pesticides", Journal of Hazardous Materials, 18(1–3), pp. 121–126, 2010. https://doi.org/10.1016/j.jhazmat.2010.04.103

[37] Zhang, G., Zhang, Q., Sun, K., Liu, X., Zheng, W., Zhao, Y. "Sorption of simazine to corn straw biochars prepared at different pyrolytic temperatures", Environmental Pollution, 159(10), pp. 2594–2601, 2011. https://doi.org/10.1016/j.envpol.2011.06.012

[38] Akram, M., Bhatti, H. N., Iqbal, M., Noreen, S., Sadaf, S. "Biocomposite efficiency for Cr(VI) adsorption: Kinetic, equilibrium and thermodynamics studies", Journal of Environmental Chemical Engineering, 5(1), pp. 400–411, 2017. https://doi.org/10.1016/j.jece.2016.12.002

[39] Khan, A. A., Mukherjee, S., Mondal, M., Boddu, S., Subbaiah, T., Halder, G. "Assessment of algal biomass towards removal of Cr(VI) from tannery effluent: a sustainable approach", Environmental Science and Pollution Research, 29(41), pp. 61856–61869, 2022. https://doi.org/10.1007/s11356-021-16102-8